

PHYSICS OF OUR DAYS

PACS numbers: 87.10.Ed, **87.16. – b**, **87.19. – j**

Calcium oscillations in blood platelets and their possible role in 'interpreting' extracellular information by cells

S S Shakhidzhanov, F A Balabin, S I Obydennyy, F I Ataullakhanov, A N Sveshnikova

DOI: https://doi.org/10.3367/UFNe.2018.05.038335

Contents

Abstract. Intracellular Ca^{2+} ions play an important role in the transmission and treatment of information that cells obtain from the ambient environment. Having received an external signal, a cell may increase the intracellular Ca^{2+} concentration within fractions of a second by a factor of several hundred. This phenomenon triggers activation of various cellular systems that generate a response to the external stimulus. In many cells under the effect of external signal the concentration of Ca^{2+} not only increases, but also starts oscillating. Both the frequency and amplitude of the oscillations are affected by the external signal strength. There are reasons to hypothesize that the conversion of the external signal into the oscillating intracellular signal has some important informational meaning. Methods to measure the dynamics of the intracellular Ca^{2+} concentration and mechanisms that generate the oscillations are reviewed, and hypotheses on how the cell decodes Ca^{2+} concentration oscillations are presented. Consideration is focused on the platelet, the cell that plays a key role in arresting hemorrhages. If a vessel is damaged, the platelet is rapidly activated. Identical platelets are divided in the process of arresting a hemorrhage into three populations with quite different missions. The platelet seems to somehow 'interpret' the set of external signals and uses the Ca^{2+} concentration oscillations to 'choose' the population to which it will belong. Owing to the platelet's relative simplicity, one can expect that studies of that cell will shortly enable the decryption of the 'code' that drives Ca^{2+} concentration oscillations.

Keywords: intracellular calcium concentration oscillations, platelets, coding, decoding, Poincaré – Andronov – Hopf bifurcation

S S Shakhidzhanov [1, 2, *], **F A Balabin** [1, †], **S I Obydennyy** [1, 3], **F I Ataullakhanov** [1, 2, 3, ‡], **A N Sveshnikova** [1, 2, 3, 4]
[1] Center for Theoretical Problems of Physicochemical Pharmacology, Russian Academy of Sciences, ul. Kosygina 4, 119991 Moscow, Russian Federation
[2] Lomonosov Moscow State University, Faculty of Physics, Leninskie gory 1, str. 2, 119991 Moscow, Russian Federation
[3] Dmitry Rogachev National Medical Research Center of Pediatric Hematology, Oncology and Immunology, ul. Samory Mashela 1, 117997 Moscow, Russian Federation
[4] I M Sechenov First Moscow State Medical University, ul. Trubetskaya 8/2, 119991 Moscow, Russian Federation
E-mail: [*] shakhidzhanov.s@yandex.ru, [†] fa.balabin@physics.msu.ru, [‡] ataullakhanov.fazly@gmail.com

Received 8 May 2018
Uspekhi Fizicheskikh Nauk **189** (7) 703 – 719 (2019)
DOI: https://doi.org/10.3367/UFNr.2018.05.038335
Translated by Yu V Morozov; edited by V L Derbov

1. Introduction

Any living system must continuously exchange energy, matter, and information with the environment — all biological systems are open. Any cell must be able not only to provide itself with vitally important energy but also to adequately respond to signals coming from the ambient environment. For this purpose the cells developed a variety of complicated mechanisms allowing them to adequately 'perceive' the environment and respond to its changes. The cell analyzes the environmental conditions by means of various receptors located on its surface, i.e., the plasma

membrane. Each receptor selectively responds to a chemical compound or impact. As soon as a signal reaches the receptor, it is transferred inside the cell to change the concentration of special substances that serve as intracellular signals or 'secondary messengers' [1]. One of such important mechanisms for the transmission of information from external stimuli into the cell is the system controlling the intracellular calcium (Ca^{2+}) level which, in turn, affects a large number of intracellular processes [3, 4]. The mechanism of external signal transport via the intracellular Ca^{2+} concentration proved so convenient and universal that many cells began to use it to obtain all kinds of environmental information, as exemplified by muscle cells [5], neurons [6], astrocytes [7], oocytes [7, 8], and various blood cells [9, 10]. In all these cells, a change in the Ca^{2+} level induces different responses: muscle cells contract, neurons are enabled to carry a signal, and blood cells become activated.

The idea that calcium can play the role of a secondary messenger dates back to 1883 when Sydney Ringer studied rat myocardium contractions [11]. Ringer first placed rat hearts into hard tap water and observed their perfect contraction. Then, he substituted tap water with distilled water, in which contractions became much weaker and finally ceased. The addition of calcium salts to distilled water restored normal cardiac contractions. Numerous experiments with various muscle tissues carried out by later researchers showed that calcium is not only necessary for their contraction but also can cause it by itself. The first experimenters used the luminescent calcium-binding protein aequorin [12] inserted into a cell by microinjection. A major breakthrough in this research area occurred in 1977 [13] when a several-fold increase in calcium concentration was recorded during oocyte fertilization. In 1980, Tsien and co-workers synthesized a number of fluorescent dyes to observe variations in calcium concentration in individual cells (see Appendix 1) [14]. Later, Woods at al. [15] found that activation of hepatic cells by external signals (hormones) not only caused a rise in the calcium level but also induced the generation of a train of very short high-amplitude pulses of Ca^{2+} concentration (Fig. 1). The frequency of these oscillations depended on signal strength. Soon after this publication, calcium oscillations were observed in cells from other organs. In became clear that the cell can respond to an external impact by producing an oscillating calcium signal of different frequency and amplitude [16]. Further studies of calcium signaling demonstrated that such oscillations constitute a universal information transmission mechanism in various cells which gave rise to a new research direction in cell biology.

The platelet is a blood cell in which an external signal causes oscillations of the calcium level. It plays a key role in the arrest of bleeding from a damaged vessel [17]. An injury to the vascular wall leads to the contact of blood with substances that activate platelets. The platelet is a relatively simple cell having neither a nucleus nor many other important systems of a normal cell. However, the platelet responses to external stimuli are quite diverse [18], which leads us to the following conclusion: the platelet not only responds uniformly to external impacts but somehow 'interprets' their spectrum and intensity. Vascular damage can be regarded as an external factor that activates platelets and enables them to perform their function. In this paper we consider problems related to the observation and interpretation of calcium oscillations in blood platelets.

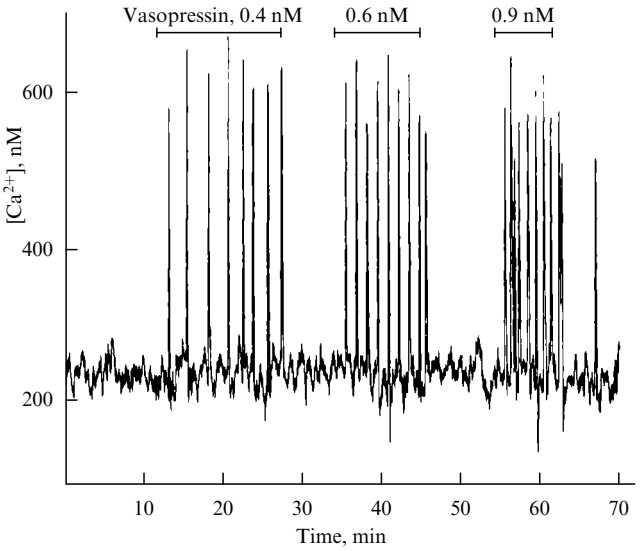

Figure 1. An example of Ca^{2+} level oscillations in hepatocytes liver cells at different concentrations of their hormonal activator (vasopressin). Intracellular calcium concentration was measured with the use of aequorin [12]. Well apparent is the periodicity of Ca^{2+} level oscillations and the dependence of their frequency on the activator level (from Ref. [15]).

2. Platelet function under complicated conditions

Platelets and thrombus. Platelets arrest a hemorrhage by forming a multicellular thrombocyte aggregate at the site of vascular damage. Special care is needed to prevent vascular occlusion by the growing aggregate that can interrupt vital oxygen supply to perivascular tissues. An additional difficulty arises from the necessity to solve this problem for vessel injuries of various sizes in different vessels with different blood flow rates. Thus far, many aspects of the mechanism underlying the growth of thrombocyte aggregates and its arrest remain obscure. Only recent studies are lifting the veil on them. We shall describe a simplified picture.

It was shown in Refs [19–23] that a thrombus has a complex structure, including an inner core and outer shell. The core contains 'strongly activated' platelets. Their main role appears to be to prevent blood loss by spreading over the damaged site and making close contact with neighboring cells. Certain platelets of the core in direct contact with the damaged site turn into the superactive 'procoagulant' state [24]. Procoagulant platelets perform a completely different function: they do not make contact with their neighbors but actively produce factors (e.g., thrombin) causing strong activation of the neighboring platelets. The core of a thrombocyte aggregate is protected from the blood flow by an envelope formed of 'weakly activated' platelets that do not make close contact between themselves and can readily detach from the aggregate. This process probably contributes to the inhibition of thrombus growth [25].

Thus, platelets are divided in the process of arresting a hemorrhage into three populations with quite different missions. Some of them produce factors activating other platelets, others prevent blood loss, while the third population protects the remaining platelets from blood flow and inhibits thrombus growth. This means that initially identical platelets contained in a thrombus undergo differentiation. Those caught up inside the thrombus or located at the damage

site must quickly identify the type to which they belong based only on information about their environment.

A platelet can 'survey' its environment using various surface receptors [26], including the binding sites for such molecules as adenosine diphosphate (ADP), collagen, and thrombin. Collagen molecules are initially 'hidden' behind the vascular wall and can be exposed to the blood flow only in case of vascular damage. Collagen-bound platelets can 'understand' that they are localized directly at the injured site. It was shown that the platelets that have bound collagen can be strongly activated as they become tightly glued together to form a thrombus core even if some of them turn into the procoagulant state. The procoagulant platelets promote thrombin production, which can cause strong activation of the next platelet layers. The strongly activated platelets together with the procoagulant ones, in turn, release ADP, which may cause slight platelet activation in the protective layer (the shell) of the thrombocyte aggregate.

On the other hand, accidental platelet activation must be prevented. For example, thrombus formation is accompanied by thrombin and ADP diffusion and/or convection due to which these molecules can be transferred far away from the thrombus. This implies the operation of mechanisms allowing such weak 'false' signals to be distinguished from valid ones; in other words, a platelet must be able to estimate the strength of external signals.

3. Phenomenon of pulsed generation of a calcium signal in platelets

3.1 Variations in Ca^{2+} concentration

Figure 2 presents video frames of thrombin-activated platelets. Ca^{2+} is visualized by fluorescence microscopy of cells injected with the vital stain Fluo 3-AM, whose fluorescence sharply increases as it binds Ca^{2+} (see Appendix 1 for details). The intensity of platelet luminescence in each frame can be compared with Ca^{2+} concentration to observe its dynamics in a single cell. Figure 3a demonstrates Ca^{2+} dynamics under the effect of a rather high concentration (10 μM) of the weak activator ADP. Platelets respond by generating a set of high-frequency and high-amplitude pulses. The signal contains a well apparent stochastic component. Figure 3b illustrates a change in the response of platelets when ADP is supplemented by the low molecular-weight peptide imitator (SFLLRN) of the part of the thrombin receptor that is liberated by thrombin, interacts with the receptor, and thereby provokes a strong response from the cell. Clearly, the activator markedly increases the repetition rate of the pulses. High concentrations of the strongest activator (thrombin) induce pulse merging (Fig. 3c) and thus maintain a practically constant Ca^{2+} high level in the cell. Thus, different, external stimuli encode oscillations of different frequencies in a platelet.

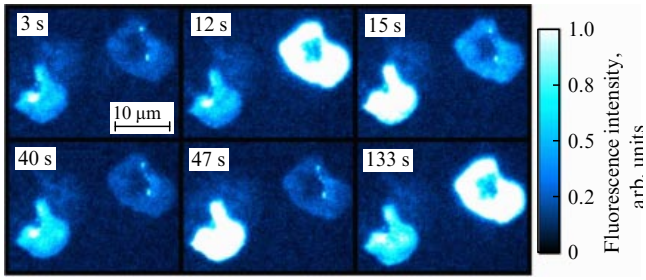

Figure 2. Platelets loaded with the Fluo 3-AM fluorescent probe. Images obtained using a Nikon Eclipse Ti-E inverted fluorescence microscope with 100×-1.49NA objective in the total internal reflection regime.

3.2 How the cell 'interprets' signals coming from the ambient environment

Any cell, including a platelet, normally contains over ten receptors of different types [17]. The number of intracellular processes that can and must change in response to external signals is also high. Surprisingly, although such external factors as ADP, collagen, and thrombin are bound by different receptors on the platelet surface, all the pathways of intracellular information transferred by these absolutely different signals eventually converge to regulate the intracellular calcium level (Fig. 4). But cells respond differently to different combinations of input signals, meaning that the calcium level dynamics encode the signals so as to enable a platelet to react differently to various external stimuli.

Nature could choose another way, namely, it could have created for each type of receptor a specific channel disjoint from others for the transfer and formation of a correct response of the cell to each of the external signals. However, it would have been a dead-end strategy, because different cell responses include a great variety of molecular and biochemical processes due to which different physiological reactions are frequently based on the same biochemical systems. Generation of a cell's physiological response involves different combinations of many molecular processes. In such a situation, it is utterly inconvenient to use a specific input signal to form each physiological response from the cell. At the same time, a certain universal intracellular signal recoding mechanism appears to be the most meaningful control method. By no means is the transfer of all signals in

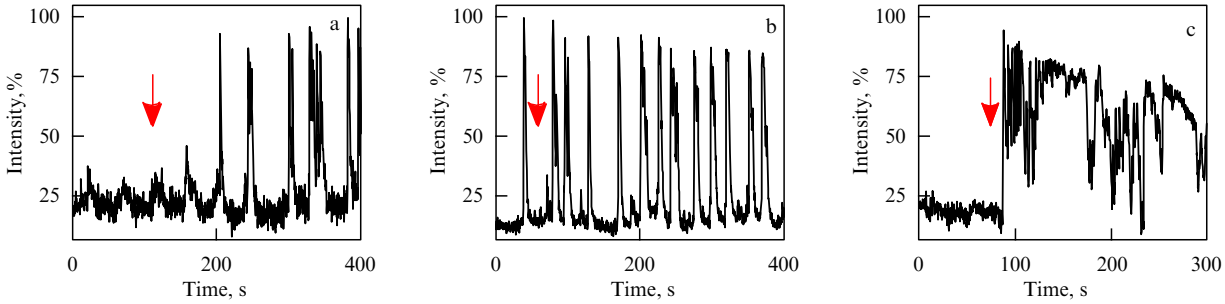

Figure 3. Calcium oscillations in a platelet in the presence of different activators. Platelet activation by 10 μM of ADP (a), 20 μM of ADP, and 3 μM of SFLLRN (b), 100 nM of thrombin (c). Arrows indicate activation time points.

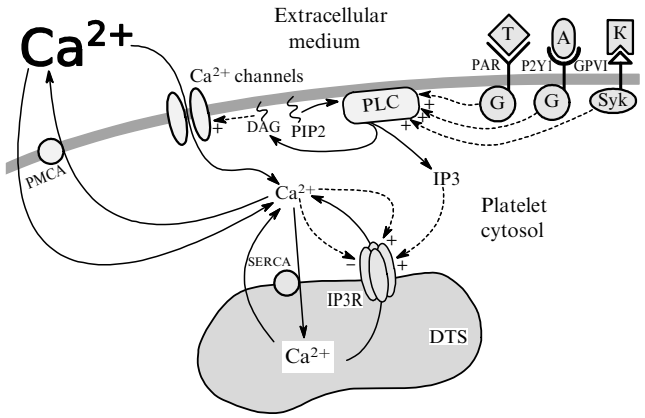

Figure 4. Calcium signaling in a platelet. Solid arrows show the direction of Ca transfer between platelet compartments and the environment. Dashed arrows indicate an activating (+) or inhibiting (−) action of the molecule. Binding of thrombin activator (T) by PAR receptors (PAR1 and PAR4) on platelets leads to their activation and signal transfer to phospholipase C (PLC) mediated through special G-proteins. Binding of a G-protein to PLC results in the cleavage of phosphatidylinositol-4,5-biphosphate (PIP2) by PLC into two signal molecules, diacylglycerol (DAG) and inositol triphosphate (IP3). PIP2 and DAG molecules remain in the plasma membrane due to the presence of hydrophobic areas. Binding of the ADP activator (A) by P2Y1 receptor also activates PLC via G-proteins. Collagen (C) binding by GPVI receptor results in the activation of a different PLC isoform via the Syk protein. IP3 binding by IP3R channels located at the membranes of one of the platelet compartments (dense tubular system, DTS) opens these channels and thereby allows calcium ions to rapidly leave the DTS down the concentration gradient. IP3R channels remain open till the concentration of calcium released from the DTS exceeds a certain critical value; they begin to close after the threshold is overcome. In the absence of an activator, calcium can slowly leak from the DTS directly across its lipid membrane. The leakage is compensated by the activity of the SERCA calcium pump that draws calcium back into the DTS. In the same way, the platelet compensates for calcium passage from the extracellular medium across the plasma membrane — the PMCA pump transports Ca into the extracellular medium. A DAG molecule can bind to different calcium channels at the outer membrane of the platelet and open them.

all cells mediated through calcium level dynamics. There are other options [27], but the recoding of input signals is beyond doubt, even though we do not perfectly understand the logic and 'language' of this mechanism.

It can be concluded based on our current knowledge that platelets use this mechanism of encoding the calcium intracellular concentration dynamics for rapid and faultless self-organization into complex thrombocyte aggregates.

3.3 Evolution of calcium signaling

Of special interest are today's concepts of the origin of calcium-mediated signal transfer in the course of evolution [28]. It seems that the primary ocean in which the first cells appeared had a low calcium concentration equaling that in all modern cells (below 5×10^{-8} M). However, it began to gradually increase in the course of time as the atmospheric CO_2 level went down and ocean water underwent acidification. In all probability, the rise in calcium concentration proved an unpleasant surprise for merely chemical reasons, taking into consideration that calcium readily binds phosphates, giving rise to insoluble compounds (by that time, phosphates had already played a very important role in natural processes). They are a part of the cell's 'energy currency', the adenosine triphosphate (ATP) molecules. Moreover, the sugar-phosphate backbone is a basis for DNA and RNA without which life would be impossible on Earth. Therefore, the first cells began to develop special protective mechanisms that pumped out calcium from cells into the environment (consuming ATP) and thereby maintained a low concentration of intracellular calcium. Moreover, it is highly possible that the increase in calcium concentration with time in cells with calcium pumps could become a marker of plasma membrane breakup requiring urgent repair; in this way, early signaling appeared. Up to now, this mechanism of information about membrane injuries operates in the simplest cells, such as erythrocytes [29], where other pathways of calcium signaling are practically nonexistent. It is surprising that the enhancement of calcium concentration in the ocean was accompanied by a growing complexity of life, including the appearance of living cells with a nucleus and the first multicellular organisms. At this stage, cells seem to have adapted to survive under conditions of a dangerously high level of calcium and taken advantage of this situation for the development of a well-controlled tool for information transmission; it promoted the further sophistication of cells and whole organisms. At present, calcium concentration in the ocean is exactly the same as in blood, i.e., 2×10^{-3} M.

4. Mathematical modeling of calcium oscillations

To date the molecular mechanisms underlying oscillations of calcium concentration in response to an external stimulus are understood fairly well. This understanding provides a basis for several mathematical models [30]. Models of calcium oscillations have been proposed for a great variety of living cells, including muscle cells [31], neurons [32], astrocytes [33], hepatocytes [34], leukocytes [35], oocytes [36], and platelets [37]. The principles of calcium concentration oscillations in these cells proved identical, even though they perform quite different physiological functions. A simplified scheme of major molecular mechanisms of calcium regulation responsible for oscillations of its intracellular level is presented in Fig. 4.

4.1 Network of biochemical reactions determining the dynamics of Ca^{2+} concentration in platelets

To ensure efficient calcium-mediated signaling, a very low calcium level (below 5×10^{-8} M) is maintained in the cytoplasm of an inactive cell, while it remains 2×10^{-3} M in the extracellular fluid [38]. Such a large gradient of calcium concentration is sustained by a special protein molecule (plasma membrane calcium ATPase, PMCA), a calcium pump continuously 'pumping' calcium out of the cell against its concentration gradient. The PMCA-pump consumes a large proportion of ATP energy generated in the cell.

Another important element of calcium signaling is the dense tubular system (DTS) [39] making up one of the intracellular compartments (a derivative of the endoplasmic reticulum) separated from the cell cytoplasm by its own lipid membrane. Different intracellular compartments enable the cell to create independent 'variously equipped laboratories' which allows separation of different (frequently interfering) metabolic processes. For example, DTS accumulates calcium that cannot remain in the cytoplasm. Calcium concentration in DTS is roughly 10^{-5} M which is three orders of magnitude higher than in platelet cytosol [39]. The lipid membrane of DTS hosts another calcium pump, sarcoendoplasmic reticu-

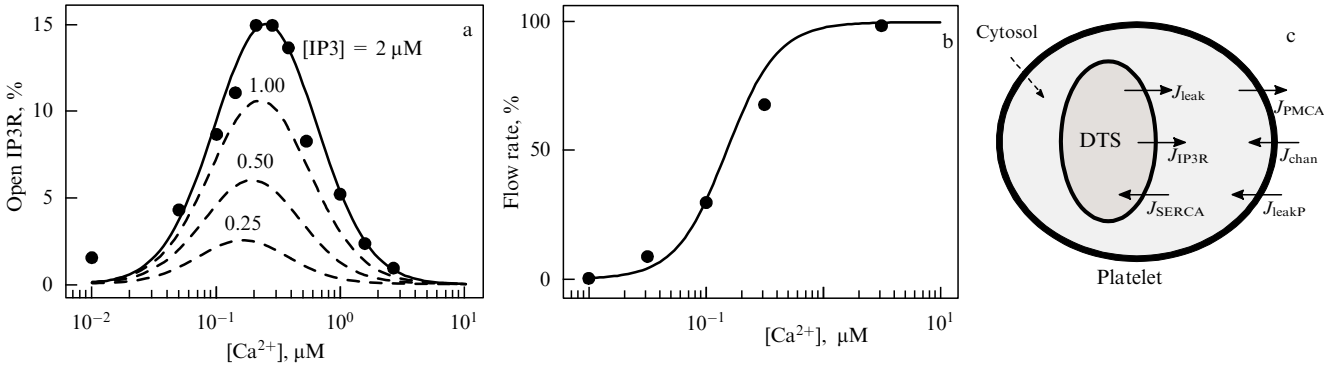

Figure 5. (a) Dependence of the equilibrium number of open IP3R receptor channels on calcium concentration in cytosol at different IP3 levels. Dots represent experimental data from [41]. (b) Calcium flow rate through SERCA pump depending on cytosol calcium level. Dots denote experimental data from [42]. (c) Directions of main calcium flows in a platelet: J_{IP3R} — mediated calcium flow, J_{leak} — calcium leakage from DTS to cytosol, J_{SERCA} — calcium flow through SERCA, J_{chan} — calcium flow through calcium channels on plasma membrane, J_{leakP} — calcium leakage from the external medium into the cytosol, J_{PMCA} — calcium flow through PMCA pump.

lum calcium transport ATPase (SERCA), which continuously pumps calcium into the DTS thus compensating its leakage from the DTS into cytosol. Also there are special receptor channels (IP3R), which are integrated into the DTS membrane; these IP3Rs are calcium channels, which can open upon the appearance of a special molecule, inositol triphosphate (IP3), in cellular cytosol. Their opening increases membrane conductivity for calcium by two or three orders of magnitude and makes it leave the DTS for cytosol along the concentration gradient. Calcium channels are also located at the outer cell membrane; they open in the presence of IP3 or diacylglycerol (DAG) in cytoplasm and let in extracellular calcium [40]. All of these factors cause a rapid increase in calcium concentration in the cytosol with characteristic times of several hundred microseconds. However, a significant rise in cytosol calcium concentration is associated with the enhanced activity of PMCA and SERCA and the IP3R channels on the contrary, begin to close (Figs 5a, b).

Thus, the appearance of IP3 and/or DAG in the cytosol can be followed by a rise in the calcium level. IP3 and DAG molecules are second messengers acting as important mediators in the transport of external signals into the cell. They can be synthesized by the special protein phospholipase C (PLC) receiving signals from different cellular receptors that trace the appearance of various signal molecules in the environment (see Fig. 4). It was mentioned above that such signal molecules for platelets are thrombin, ADP, and collagen. There is a special receptor for each of them, namely, the protease-activated receptor (PAR1) for thrombin, the purinoreceptor 1 (P2Y1) for ADP, and the glycoprotein VI (GPVI) receptor for collagen [27].

4.2 Simple mathematical model of Ca^{2+} dynamics in the cell

Based on the described molecular processes one can formulate the basic mathematical model of Ca^{2+} concentration dynamics in the cell. Figure 5c shows Ca^{2+} flows in this model. Let c be the cytosol calcium level, c_e the calcium concentration in DTS, and p the IP3 concentration. Let us then consider two IP3R states, open and closed for calcium passage. h and $1-h$ stand for the fractions of closed and open receptors, respectively. Calcium can leave the DTS through the IP3R channels (J_{IP3R}) and, in a smaller amount, through the plasma membrane (J_{leak}). Calcium is pumped into the DTS by the SERCA (J_{SERCA}), while the PMCA pump removing calcium from the cell creates a J_{PMCA} flow. Calcium can enter a platelet from the outside through various calcium channels J_{chan} and owing to leakage J_{leakP}. Transitions of receptor channels J_{IP3R} between open and closed states, i.e., quantity h, are described by a complicated function f depending on calcium and IP3 cytoplasm levels. If the ratio of the cytosol volume to that of the DTS is denoted by γ, the following set of equations can be derived to describe cytosolic calcium dynamics:

$$\frac{dc}{dt} = J_{IP3R}(c, c_e, h, p) + J_{leak}(c, c_e) - J_{SERCA}(c, c_e) + J_{chan}(c, p) - J_{leakP}(c) - J_{PMCA}(c), \quad (1)$$

$$\frac{dc_e}{dt} = -\gamma\left[J_{IP3R}(c, c_e, h, p) + J_{leak}(c, c_e) - J_{SERCA}(c, c_e)\right], \quad (2)$$

$$\frac{dh}{dt} = f(c, h, p). \quad (3)$$

A few simplifications facilitate modeling and interpretation of simulation results. First, IP3R concentration can be regarded as three-dimensional, notwithstanding that the receptors are located on the membrane, i.e., a 2D surface. Such an approximation can be deemed reasonable because the DTS membrane has many alternate protrusions and recesses [17], so that the distribution of membrane IP3R channels in the cytosol is practically uniform. Also, the SERCA and PMCA pumps as well as other membrane proteins can be considered as uniformly distributed in the cytosol.

Moreover, Eqns (1)–(3) were derived on the implicit assumption that Ca^{2+} ions in small cells have enough time to be mixed up perfectly well by diffusion inside different compartments. From calcium intracellular diffusion coefficient $D = 5.3 \times 10^{-6}$ cm^2 s^{-1} [43], one can estimate that the approximation of a well mixed medium in a platelet holds for processes with characteristic times on the order of 5–50 ms. Because the characteristic time of calcium concentration oscillations in a platelet exceeds 1 second, calcium diffusion in the cell can be neglected.

Also, assume that a platelet is closed to calcium, which can neither enter nor leave it. It seems to be a sensible approximation bearing in mind that the form of oscillations in the case of

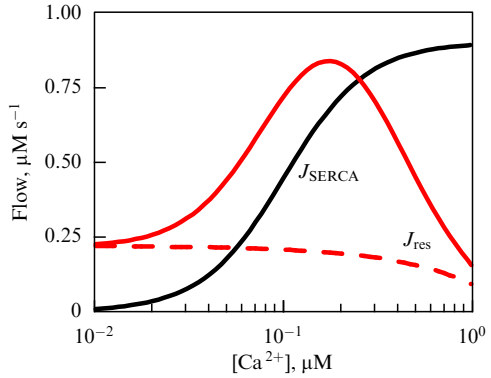

Figure 6. (Color online.) Simplest model (4), (5) of calcium concentration oscillations in which the external signal controls oscillation amplitude. Dependence of stationary flow rates $J_{res} = J_{IP3R} + J_{leak}$ (red curve) and J_{SERCA} (black curve) on calcium concentration in the cytosol. J_{res} flow is shown for two IP3 levels: 0 (dashed curve) and 0.5 μM (solid curve). At any level of IP3, the dependence for J_{res} has a single point of intersection with J_{SERCA} at any IP3 concentration at which calcium pumping out of and back into the DTS occurs at equal rates (equilibrium position).

moderate activation over long enough time intervals can remain virtually constant if the operation of both PMCA and calcium channels on the outer cell membrane is completely blocked [44]. All changes in the cytoplasm Ca^{2+} level are due to calcium redistribution between the cytoplasm and DST. Then, $J_{chan} = J_{leakP} = J_{PMCA} = 0$, and, therefore, the law of conservation of matter holds true: $dc/dt = -\gamma^{-1}(dc_e/dt)$. Thus, the c_e level can be expressed as $c(t) + c_e(t)/\gamma = \text{const} = c_{tot}$, where c_{tot} is the total calcium concentration in a platelet. Function $f(c, h, p)$ is expressed explicitly. In this case,

$$\frac{dc}{dt} = J_{IP3R} + J_{leak} - J_{SERCA}\,, \tag{4}$$

$$\frac{dh}{dt} = \frac{h_\infty - h}{\tau_h}\,, \tag{5}$$

where

$$J_{leak} = v_2\left[c_{tot} - (1+\gamma^{-1})c\right], \quad J_{SERCA} = \frac{v_3 c^2}{K_3^2 + c^2}\,,$$

$$J_{IP3R} = v_1 m_\infty^3 h^3\left[c_{tot} - (1+\gamma^{-1})c\right],$$

$$m_\infty = \frac{pc}{(p+d_1)(c+d_5)}\,, \quad h_\infty = \frac{Q_2}{Q_2 + c}\,,$$

$$\tau_h = \frac{1}{a_2(Q_2 + c)}\,, \quad Q_2 = \frac{p + d_1}{p + d_3}\,d_2\,,$$

$v_1 = 6\ \text{s}^{-1}$, $v_2 = 0.11\ \text{s}^{-1}$, $v_3 = 6\ \text{s}^{-1}$, $c_{tot} = 2\ \mu\text{M}$, $\gamma^{-1} = 0.185$, $K_3 = 0.1\ \mu\text{M}$, $d_1 = 0.13\ \mu\text{M}$, $d_2 = 1.049\ \mu\text{M}$, $d_3 = 0.9434\ \mu\text{M}$, $d_5 = 0.08234\ \mu\text{M}$, $a_2 = 0.2\ \mu\text{M}^{-1}\ \text{s}^{-1}$.

The set of equations (4), (5) comprehensively describes calcium concentration dynamics in a cell closed to calcium [45]. Figures 6–9 illustrate the dynamics of calcium behavior in the model. Figure 6 shows dependences of calcium stationary flow entering the cytoplasm, $J_{res} = J_{IP3R} + J_{leak}$, and its outflow back into the DTS, J_{SERCA}, on the cytoplasm calcium level. These dependences have a single intersection point at which the rates of calcium outflow from the DTS and its pumping back into this system are equal, i.e., the system is

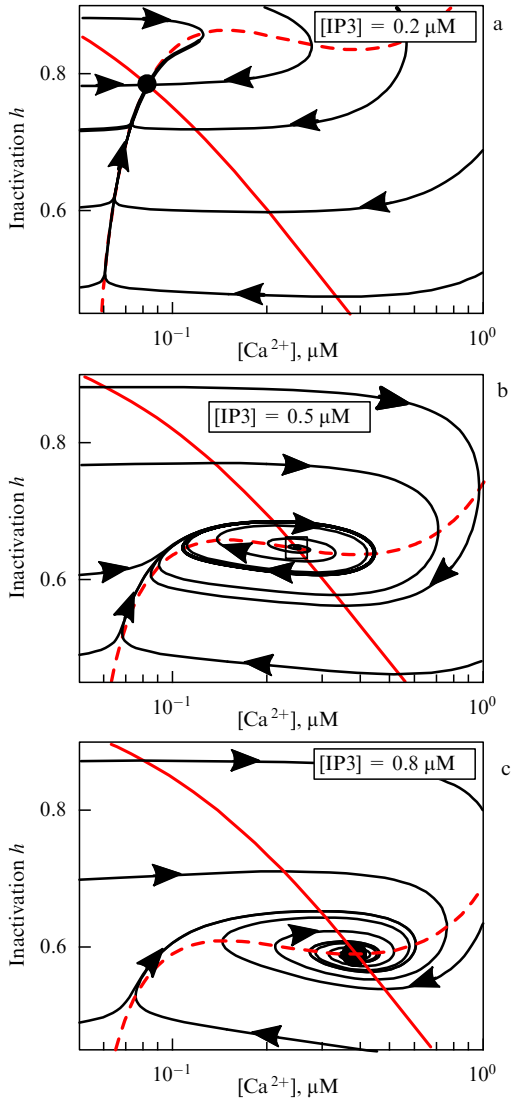

Figure 7. (Color online.) Simplest model (4), (5) of calcium concentration oscillations, in which an external signal controls oscillation amplitude. Phase portraits of the system at different IP3 levels in the cytosol. Black curves with arrows — trajectories of the system motion, red dashed curve — $dc/dt = 0$ isocline, red solid curve — $dh/dt = 0$ isocline. At 0.2 μM IP3 (a), the system has a single equilibrium position (stable node); at 0.5 μM IP3 (b), the stable limit cycle is realized; at 0.8 μM IP3, the system displays a stable focus.

in equilibrium. Set of equations (4), (5) is two-dimensional, which means that the phase space is a plane. Figures 7 and 8 show phase portraits and calcium level dynamics in this system at different IP3 concentrations. The system's isocline $dc/dt = 0$ is N-shaped. At a low IP3 concentration, isocline $dh/dt = 0$ crosses the ascending part of $dc/dt = 0$ isocline. In this case, their intersection point, which is a singular point of the system, represents the stable equilibrium position. Therefore, oscillations are absent at low IP3 concentrations, but single peaks of calcium concentration may appear. At a certain instant during the growth of IP3 concentration, the $dh/dt = 0$ isocline begins to cross the descending part of $dc/dt = 0$, resulting in a Poincaré–Andronov–Hopf bifurcation (PAHB) (see Appendix 2) and causes soft excitation of undamped oscillations of calcium concentration: a limit cycle develops in the system (see Fig. 9). The oscillation amplitude increases with IP3 concentration till isocline $dh/dt = 0$

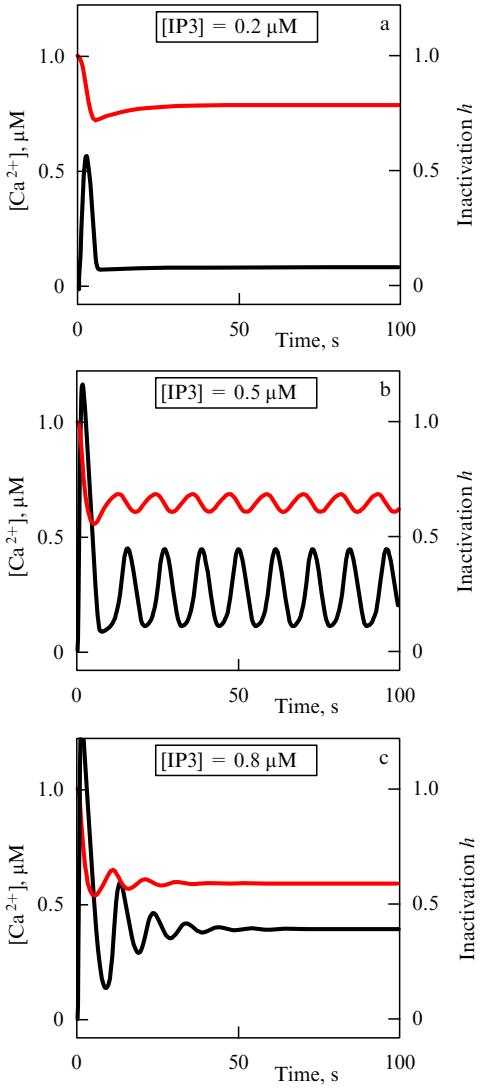

Figure 8. (Color online.) Simplest model (4), (5) of calcium concentration oscillations in which an external signal controls the oscillation amplitude. Dynamics of calcium concentration in time (black curve) and variable h denoting IP3R inactivation in time (red curve) at different IP3 levels: 0.2 μM (a), 0.5 μM (b), and 0.8 μM (c).

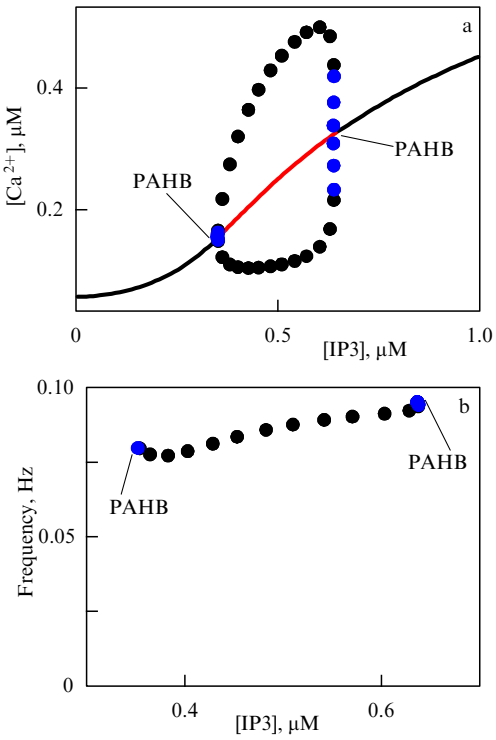

Figure 9. (Color online.) Simplest model (4), (5) of calcium concentration oscillations in which an external signal controls the oscillation amplitude. Bifurcation diagrams. Solid black curve — stable equilibrium position of the system, red curve — unstable equilibrium position, blue circles — amplitude of unstable calcium oscillations, black circles — stable oscillation amplitude. (a) A rise in IPR3 concentration is associated with Poincaré–Andronov–Hopf bifurcation (PAHB) when the stable point becomes unstable, the limit cycle develops, and soft excitation of oscillations takes place. A further rise in IP3 concentration amplifies oscillations and the limit cycle increases in size. At a certain IP3 level, another PAHB occurs that transforms the stable limit cycle into the stable focus. (b) Calcium oscillation frequency depending on IP3 level (it varies insignificantly).

intersects the ascending part of $dc/dt = 0$ again. Then, another bifurcation develops, and the limit cycle disappears, being substituted by a stable focus, and the oscillations damp out. All this makes possible stable oscillations of the calcium level in the system under consideration within a certain IP3 concentration range.

4.3 Threshold behavior of the system

Worthy of note is an important feature of the simplest calcium level control model. The model predicts that a rise in the IP3 concentration up to the level associated with bifurcation does not significantly alter the stationary Ca^{2+} concentration in the cell. A jumpwise change in the cell state occurs only after the threshold IP3 level is reached. The stationary state gives way to the nonstationary one, and the developing oscillations of calcium concentration result in its significant short-term increase in the cytosol. This mechanism is similar in the nature to an 'all-or-none' response, suggesting that the cell totally disregards a low activator level, but abruptly changes the character of its own response to an external signal when bifurcation occurs after a certain threshold concentration of the activator is exceeded. From what is known about molecular mechanisms of signal transfer in the cell described in Section 3, it can be deduced that IP3 production in the cell is triggered by the appearance of a certain external activator. This suggests that the cell does not react to some range of activator levels in the cytosol within which the activator fails to increase the calcium concentration. Oscillations cease at a very high concentration of the activator when the calcium concentration rises to a new stably high stationary level.

The mechanism underlying initiation of Ca^{2+} concentration oscillations via PAHB was described for the first time in [46]. Later investigations confirmed that it operates in many cells [30].

4.4 How the cell controls the Ca^{2+} oscillation frequency

The main disadvantage of the simple calcium oscillation model is the absence of a relationship between the oscillation rate and IP3 concentration (Fig. 9b). The character of bifurcations and oscillations may be quite different if the above description of the work of the calcium pump is incorrect. This description is based on a protein extracted from the cell. In vivo pump operation may be somewhat different, namely, a variety of proteins may contribute minor changes to the operation of SERCA pump. The phase

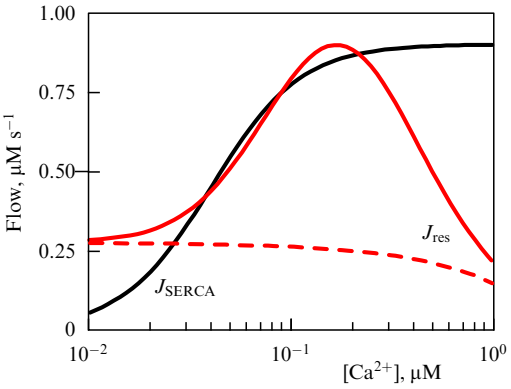

Figure 10. (Color online.) Model of calcium concentration oscillations in which the external signal controls the oscillation frequency. Dependences of stationary flow rates $J_{res} = J_{IP3R} + J_{leak}$ (red curves) and J_{SERCA} (black curve) on calcium concentration in cytosol. J_{res} flow is shown for two IP3 levels: 0 (dashed curve) and 0.4 μM (solid curve). The change in parameter K_3 shifts J_{SERCA} dependence to the left (black curve) with respect to dependence J_{SERCA} in Fig. 6. This gives rise to two more intersection points.

portrait of the system can be altered significantly upon a minor change to parameter K_3 responsible for SERCA operation [45]. At $K_3 = 0.04$ μM, the J_{SERCA} dependence is shifted to the left, which leads to the appearance of three singular points instead of one (Fig. 10), markedly altering the calcium concentration dynamics. At the beginning, when the IP3 level is as low in this system as in the preceding one, there is an equilibrium position in which the $dh/dt = 0$ isocline intersects the ascending part of the N-shaped isocline which makes such a position stable (Figs 11, 12). Here, individual calcium concentration peaks can appear too.

A rise in the IP3 level is associated with bifurcation of the creation of a pair of singular points: a saddle and an unstable focus appear. However, this does not affect the stability of the system as a whole, because the pre-existing singular point is preserved and the system remains in a single stable equilibrium position characteristic of all system trajectories. As the IP3 level continues to increase, this stable singular point gradually shifts to the right and passes through a maximum at the N-shaped isocline $dc/dt = 0$; thereafter, it begins to cross the descending part of this isocline. The equilibrium position loses stability when the singular point goes through the maximum. A complex bifurcation of the creation of a large stable limit cycle occurs. This cycle involves the region of existence of two unstable factors separated by a saddle, i.e., encompasses all three special points at a time. The system undergoes hard excitation of high-amplitude oscillations. The character of motion in the limit cycle is strongly nonlinear. The system slowly moves along the left branch of the isocline, which corresponds to a low Ca^{2+} concentration and slow pore opening in DTS. The trajectory breaks down after the isocline maximum is reached: Ca^{2+} concentration begins to grow rapidly, reaches a maximum, and quickly decreases till the trajectory comes back to the left branch of the isocline. Thus, a characteristic Ca^{2+} response is formed that consists of a short high-amplitude impulse followed by a long time interval during which the Ca^{2+} concentration is very low.

As the IP3 level continues to grow, the right unstable point moves toward the right, ascending part of the $dc/dt = 0$ isocline. At this moment, one more PAHB occurs and an unstable cycle forms within the stable limit cycle. It grows in

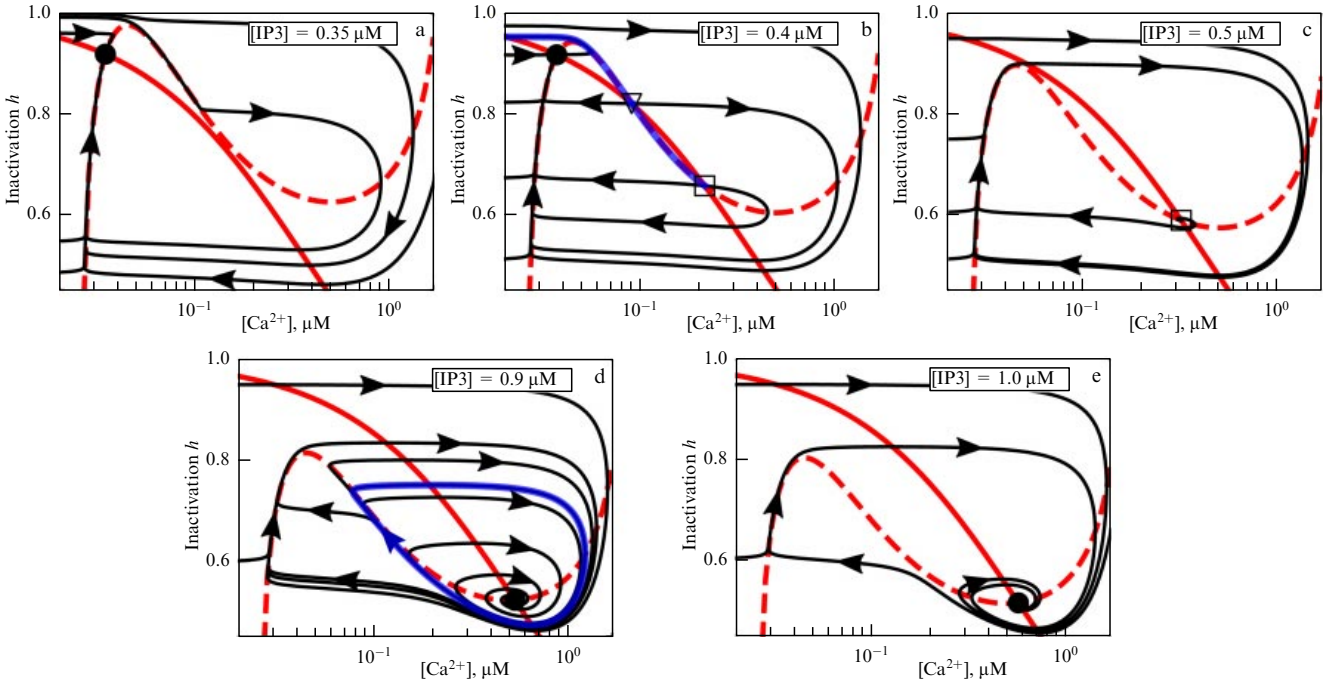

Figure 11. (Color online.) Model of calcium concentration oscillations in which an external signal controls the oscillation frequency. Phase portraits of the system at different cytosol IP3 levels: 0.35 μM (a), 0.4 μM (b), 0.5 μM (c), 0.9 μM (d), and 1.0 μM (e). Black curves with arrows — system movement trajectories, red dashed curve — $dc/dt = 0$ isocline, red solid curve — $dh/dt = 0$ isocline. At 0.35 μM IP3 (a), the system has a single equilibrium position (stable node). At 0.4 μM IP3 (b), two more singular points appear: a saddle (triangle) and an unstable node (square). Separatrix (blue curve) depicts incoming saddle branches. As the IP3 level increases to 0.5 μM (c), two singular points disappear and only the unstable focus remains, around which a stable limit cycle forms. At 0.9 μM (d), the system has two limit cycles, with the unstable one represented by a separatrix (blue curve) arising inside the stable one. Only the latter remains at 1.0 μM.

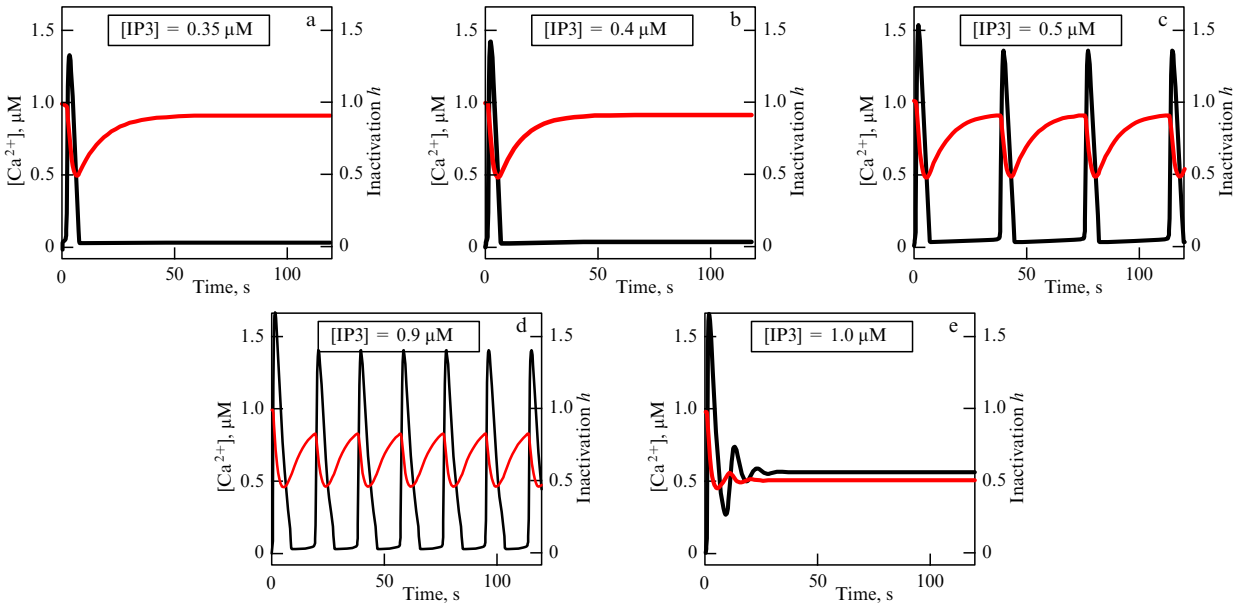

Figure 12. (Color online.) Model of calcium concentration oscillations in which the external signal controls the oscillation frequency. Dynamics of calcium concentration (black curve) and variable h denoting IP3R inactivation (red curve) in time at different IP3 levels: 0.35 μM (a), 0.4 μM (b), 0.5 μM (c), 0.9 μM (d), and 1.0 μM (e).

size until it entraps the stable limit cycle, and only the stable focus remains in the system, while calcium level oscillations decay.

The calcium concentration dynamics being considered is radically different from that shown in Figs 6–9. First, the hard excitation of calcium level oscillations takes place in this case. Second, the amplitude of calcium oscillations remains unaltered, unlike the oscillation frequency, which changes (Fig. 13b). The former difference relates to the hard excitation of oscillations, the latter one to the rise in IP3 concentration leading to a size reduction in the ascending part of the $dc/dt = 0$ isocline (upward-directed trajectories in the left part of Figs 13a, b) over which the slowest movement of the system trajectories takes place.

4.5 Stochastic component of Ca^{2+} oscillations

A comparison of theoretical (see Fig. 12) and experimental oscillations reveals a considerable difference. Oscillations occur in both cases, but the model predicts regular oscillations with a constant amplitude and frequency, whereas experiments demonstrate their marked stochasticity, especially in the system's response to weak activators. Experimental data do not permit the amplitude and frequency of calcium level oscillations to be unambiguously determined; they seem random. The conventional explanation for calcium oscillation stochasticity in a platelet is that it is small in volume ($\sim 10^{-15}$ l) and therefore poor in ions (normally, such a volume contains about 50 calcium ions). Such a small number of ions can account for fluctuations affecting the oscillation dynamics. Therefore, one cannot model such processes with the use of ordinary differential equations. They are described by stochastic equations. The Gillespie algorithm [47] allows obtaining a statistically valid trajectory (one of the possible solutions of the fundamental kinetic equation) for a stochastic equation. The physical basis of the algorithm is molecular collisions in a reactant-containing vessel. The algorithm selects, on the assumption of the probability of such collisions, a reaction that must occur at a certain point in time. If the probability of 'molecular collisions' is specified in terms of flows as in system of equations (4), (5), modeling can yield a set of calcium level trajectories at different IP3 concentrations. Two typical trajectories are presented in Fig. 14. Evidently, the results of calculations agree with experimental data. However, such stochastic oscillations of calcium concentration are not observed in large cells. Moreover, it is presently believed that cells tend to suppress dynamic chaos that may occur in their metabolic systems [48].

4.6 Detailed modeling of Ca^{2+} dynamics in the cell

It was mentioned in Section 4.2 that the results presented in Figs 6–14 were obtained based on certain assumptions. For example, we suggested that the cell is closed to calcium. Also, we used a simplified equation describing the dynamics of the IP3R channel opening and closing (h dynamics). Today, it is generally accepted that the IP3 receptor can be in six different states, changing from one to another depending on calcium and IP3 levels. One such model allowing for the complicated dynamics of IP3R transitions and cell openness for calcium is described in Appendix 3. However, the main features of calcium concentration dynamics are preserved in this intricate model characterized by a PAHB-related oscillation generation threshold. This model also involves hard excitation of calcium level oscillations, and a rise in the IP3 level results in an increase in their frequency even more stronger than that shown in Fig. 13. Moreover, cells were shown to possess positive and negative feedback able to change the shape of calcium concentration oscillations [49].

Another approximation relates to rapid equalization of concentrations in the entire cell as a result of fast calcium diffusion in the cytosol. This approximation, justified for platelets and other small cells, is inapplicable to bigger cells, such as neurons and oocytes, in which calcium level oscillations also occur. The activation region in these cells is inherently small. For example, activation in a large oocyte is triggered by a small spermatozoon penetrating into a small

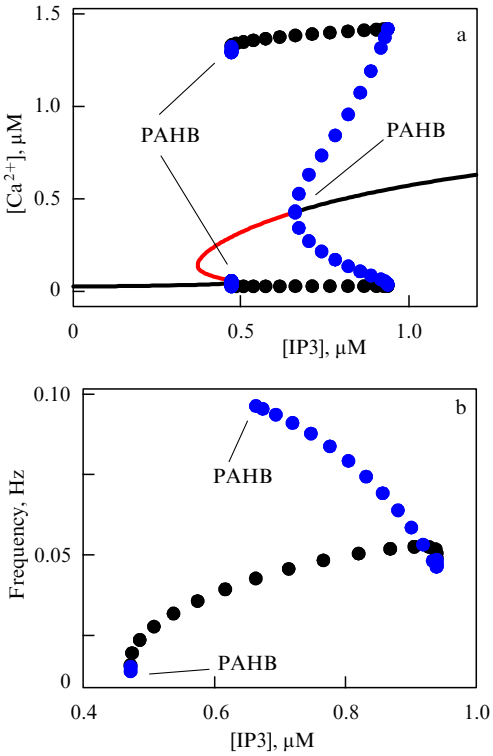

Figure 13. (Color online.) Model of calcium concentration oscillations in which the external signal controls the oscillation frequency. Bifurcation diagrams. Solid black curve shows stable equilibrium position of the system, red curve unstable equilibrium position blue dots the amplitude of unstable calcium oscillations, black dots the stable oscillation amplitude. (a) A rise in the IP3 level is associated with the formation of two unstable states followed by Poincaré–Andronov–Hopf bifurcation and hard excitation of calcium level oscillations, with their amplitude remaining practically unaltered. At a certain IP3 level, another PAHB takes place, and an unstable limited cycle develops within the stable one. The former expands until it completely encompasses the latter, and only the stable focus remains in the system. (b) Calcium oscillation frequency increases with increasing IP3 level.

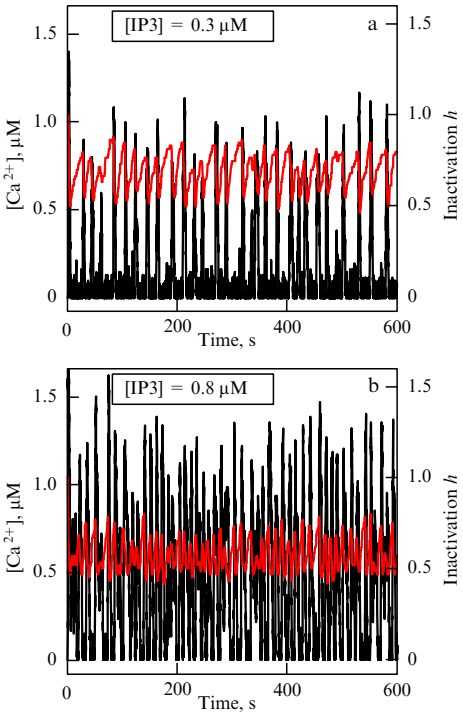

Figure 14. (Color online.) Model of calcium concentration oscillations in which the external signal controls the oscillation frequency. Stochastic simulation of calcium concentration oscillations in the simplest model by the Gillespie method [47]. Because of a very low number of free calcium ions in a nonactivated platelet (around 50), fluctuations of calcium concentration in the cytoplasm cause its abrupt changes, even at as low an IP3 level as 0.3 μM (a). The frequency of such jumps increases as the IP3 level rises to 0.8 μM (b). The black curve shows Ca^{2+}concentration, the red one receptor inactivation *h*.

part of the oocyte. Neuron activation is induced by a process of another neuron connected to the former through a small synapse. A fine outcome of calcium level oscillations in big cells is the generation of spatial autowaves of calcium concentration; the self-sustaining waves of calcium concentration begin to propagate from the activation site to all parts of the cell, where they alternately open and close IP3R channels. The reader is referred to [50] for a detailed description of this perfect result.

5. Decoding the calcium signal in a cell

Both mathematical models and experiments show how various agonists can induce calcium level oscillations of various frequencies in biological cells. Everything depends on the level of IP3 produced by PLC. A rise in the IP3 concentration induces threshold initiation of calcium oscillations with the frequency and amplitude dependent on the IP3 level. As is shown above (see Fig. 4), platelets have collagen, ADP, and thrombin receptors that transmit the activating signal to PLC (Fig. 4), but signals transferred by each of these receptors differ in strength. Therefore, each extracellular signal induces calcium level oscillations of various frequencies, enabling a platelet to distinguish among ADP, collagen, and thrombin and simultaneously filter out weak signals. The literature gives evidence that platelets express one order of magnitude more PAR1 than P2Y1 [17]. Probably, due to this, signals from thrombin receptors are much stronger than those from ADP receptors.

The cell, however, must convert a pulsed signal into the activation of proper proteins to be able to adequately react to the stimulus. How the cell copes with this task (especially under stochastic oscillation conditions) remains to be understood. Let us consider current hypotheses of the Ca^{2+} signal decoding mechanism.

Protein kinase C (PKC) is one of the proteins capable of decoding calcium concentration oscillation frequency [51, 52]. It can affect the activity of other proteins by their covalent modification, i.e., it covalently attaches phosphate to their specific amino acids and thereby either inhibits or activates them [53]. PKC has an intricate structure (Fig. 15a), including two domains for binding calcium and DAG, respectively, the latter molecule being produced by PLC simultaneously with IP3. To become active and capable of modifying other proteins, PKC must covalently bind both calcium and DAG. Calcium is to be bound first, because the binding site for DAG becomes available only after PKC bounded calcium. Calcium binding with its specific domain on PKC occurs rather rapidly when its cytosol concentration increases. Conversely, a decrease in calcium concentration stimulates its fast release from the binding domain. The coupling between PKC and calcium opens the DAG domain and DAG begins to slowly bind to it. Although the process is

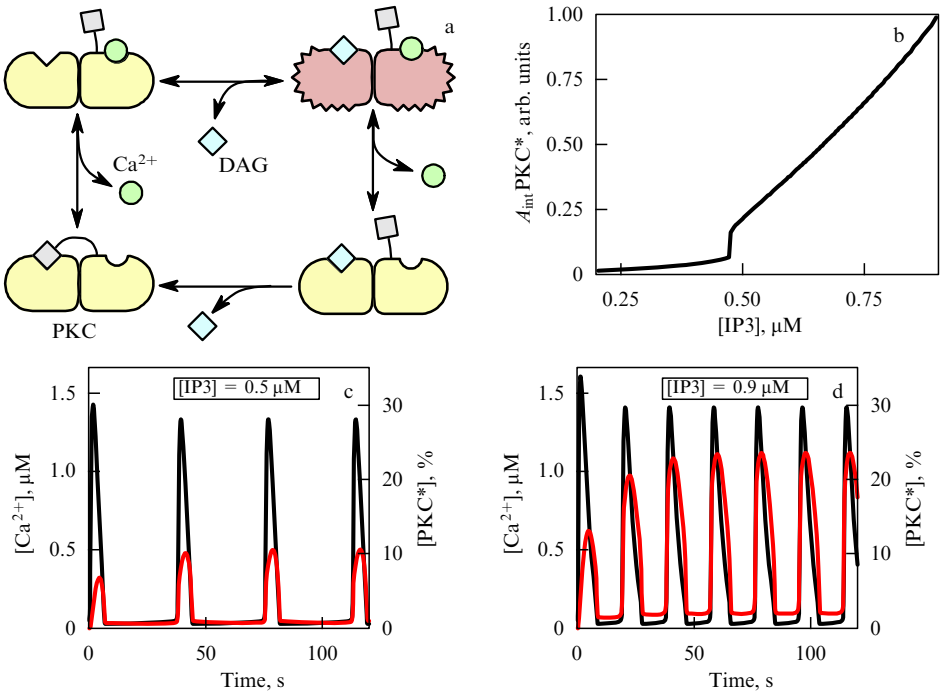

Figure 15. (Color online.) Decoding calcium concentration oscillation frequency using PKC protein (a). Schematic of PKC activation. Non-activated PKC is indicated by the yellow color, activated PKC by the red color. PKC* stands for activated PKC with bound Ca and DAG. PKC has two domains for binding Ca and DAG, respectively. The DAG-binding domain is closed till PKC binds Ca. PKC becomes active only if both Ca and DSG are bound to it. DAG remains attached to its binding domain of activated PKC for some time after calcium is released. However, this protein cannot bind a new DAG molecule in the absence of bound calcium because its DAG-binding domain is closed. It opens only after the binding of calcium by PKC. However, DAG binding is a rather slow process. As the cytosol Ca level decreases, calcium detaches from PKC, whereas DAG detachment occurs later. A rise in calcium concentration in the cytosol promotes rapid recovery of PKC activity. (b) PKC integral activity (A_{int}) depending on IP3 level deduced from the calcium concentration oscillation model predicting frequency modulation (c, d). Examples of PKC activation dynamics at IP3 levels of 0.5 μM (c) and 0.9 μM (d).

slow, the binding is very strong and persists for some time after the Ca^{2+} concentration decreases and its ions detach from the binding domain. If calcium concentration increases again at this instant, its ions go back to the respective binding domain of PKC that becomes activated. However, if PKC loses DAG by this time, the DAG-specific domain closes and activation has to be started from the beginning including calcium binding and slow attachment of DAG. Such a property of PKC makes its activity susceptible to the frequency of calcium level oscillations.

This means that in the case of sufficiently frequent calcium level oscillations, PKC occurs mainly in the activated state, whereas the inactivated enzyme prevails in the case of rare calcium oscillations. The IP3 dependence of PKC integral activity at frequency-modulated calcium level oscillations is illustrated by Fig. 15b. The figure shows that the integral PKC activity increases linearly with IP3 concentration. Examples of PKC activation dynamics at different IP3 levels are presented in Figs 15c, d.

Another protein sensitive to Ca^{2+} level oscillation frequency is Ca- and DAG-regulated guanine-nucleotide exchange factor I) (CalDag-GEF-I) [54, 55]. Despite its name, the activity of this protein does not depend on DAG, but depends on calcium concentration. It operates together with two other proteins, Ras-related protein 1 (Rap1) and GTPase-activating Rap1 protein (Rap1-GAP2) (Fig. 16a). Rap1 acts as a switch capable of activating other proteins. Switched-off Rap1 binds guanosine diphosphate (GDP). CalDag-GEF1 has a binding domain for calcium; it is activated when calcium concentration increases. Activated CalDag-GEF1 binds Rap1-GDP and substitutes GDP with guanosine triphosphate (GTP) in this protein. Switched-on Rap1-GTP begins to affect the activities of other proteins. Rap1-GAP2 can bind Rap1-GTP and switch it off by substituting GDP for GTP.

At rare calcium concentration oscillations, CalDag-GEF-I activity can be compensated by that of Rap1-GAP2. But at sufficiently frequent oscillations, Rap1-GAP2 has no time to switch off CalDag-GEF-I, and Rap1 begins to be gradually activated. The integral activity of Rap1-GTP depending on IP3 concentration for frequency-modulated oscillations of the calcium level is shown in Fig. 16b. Figures 16c, d illustrate Rap1 activation dynamics at different IP3 concentrations. Both examples reveal a similar Ca^{2+} concentration dependence, but the latter one suggests the involvement of many various proteins and metabolic systems in the response to variations in the Ca^{2+} level.

Intracellular mitochondria can just as well participate in decoding calcium concentration oscillations [56, 57]. These cell compartments contain special pumps to bring calcium into the cell. The mitochondrial calcium level influences energy (ATP) production in the cell. An interesting feature of mitochondria is excessive calcium accumulation at a very high frequency (and possibly amplitude) of Ca^{2+} level oscillations [37, 58]. It results in their overload and arrest of energy production. Apparently, this is a transition into the third (procoagulant) state [59, 60], in which the cell is on its way to death. It swells out in a spherical shape and loses asymmetry of molecule distribution in the membrane. This activates the final stages of thrombus formation and arrests its growth. To date this is the most poorly studied stage of the blood coagulation process.

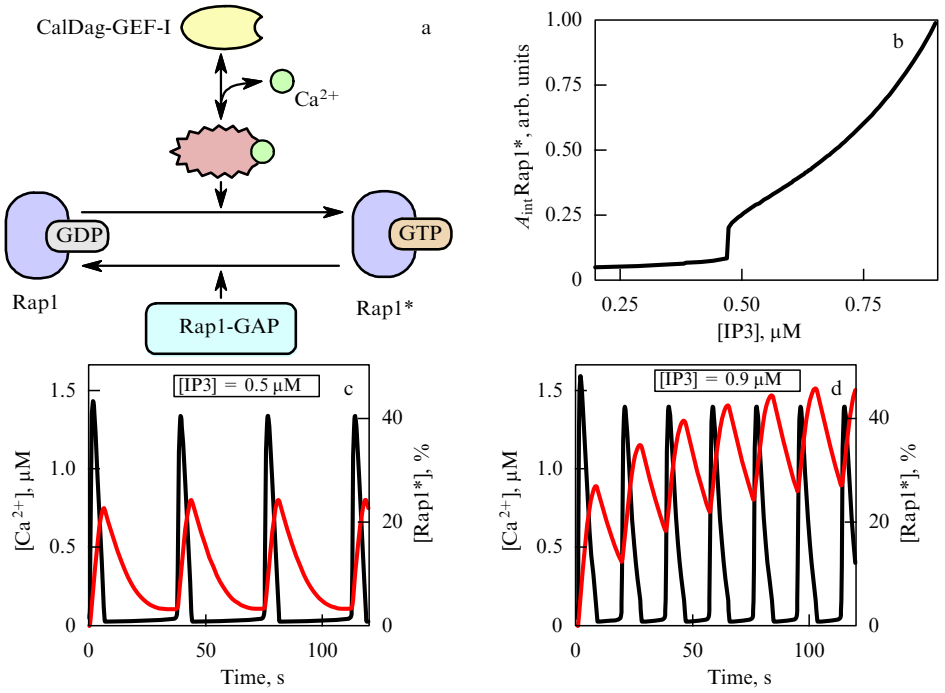

Figure 16. (Color online.) Decoding calcium concentration oscillation frequency by means of CalDag-GEF-I. (a) Schematic of Rap1 activation. Initially, Rap1 is switched off. In this state, it is bound to GDP. CalDag-GEF-I has a calcium-binding domain. Inactive CalDag-GEF-I (yellow color) can bind calcium and undergo activation (activated CalDag-GEF-I is indicated by red color). Activated CalDag-GEF-I can activate Rap1 by substituting GTP for GDP. Rap1-GAP is invariably active; it inactivates Rap1-GTP by substituting GDP for GTP. (b) Integral activity (A_{int}) of Rap1-GTP (denoted by Rap1*) depending on IP3 concentration. The calcium concentration oscillation model giving frequency modulation (c, d) is used. Examples of Rap1 activation dynamics at IP3 levels of 0.5 μM (c) and 0.9 μM (d).

6. Conclusions

Activation of blood platelets is accompanied by oscillations of cytosolic concentration of calcium ions that transfer information from the plasma membrane into the cell. Penetration of calcium ions into the platelet cytosol induced by cell surface receptors is the central activation event. An interesting feature of platelets is that almost all external signals converge on a single intracellular receiver, the calcium oscillation generating system. The total strength of input signals is transformed into a roughly proportional increase in the oscillation frequency. Recent progress in biochemistry and microscopy made possible high-resolution observations of calcium concentration oscillations in isolated platelets. The analysis of oscillation development mechanisms by nonlinear dynamics methods indicates that cells possess a special dynamic oscillator inducing hard excitation of oscillations, which accounts for the threshold response of the cells representing their very important biological property that allows them to disregard accidental fluctuations. Another peculiarity of this dynamic system is that hard excitation of oscillations causes an almost linear increase in oscillation frequency in response to the strengthening of input signals. In turn the successive rise in the oscillation frequency in response to increasingly stronger activating signals enables a cell to sequentially involve the growing number of different systems needed for the reliable performance of the blood coagulation system.

Acknowledgements. The authors are grateful to M A Panteleev, V V Mustyatsa, and A A Mart'yanov for the helpful discussions of this study. It was conducted with the application of research facilities of the Centre for Collective Use of High Performance Computing Resources, M V Lomonosov Moscow State University. The work was supported by the Russian Science Foundation (grant 17-74-20045).

Appendix 1. How to monitor calcium concentration in a platelet

At present, the fluorescence microscope is the most precise and convenient tool for observing variations in calcium concentration in platelets. Modern fluorescence microscopes make use of epi-illumination, allowing the excitation light to illuminate a sample through the same objective that is employed to visualize fluorescent emission. Fluorescence excitation and emission are separated by a dichroic mirror that reflects short-wavelength exciting light but transmits the long-wavelength fluorescence light to the video camera (Fig. 17a). Modern dichroic mirrors are of amazingly high quality. They separate two wavelengths differing only slightly (100 nm) from each other with practically 100% efficiency. Considerable progress in the performance of fluorescence microscopes is due to the use of lasers for exciting fluorescence and the advent of stable ultrasensitive charge-coupled devices (CCDs). However, all these advantages of microscopes would be of little value in the absence of a probe, e.g., a molecule capable of entering a cell and binding Ca with the resulting change in fluorescence. It became possible to observe changes in calcium concentration in individual cells only after the invention of fluorophores, such as the Fura-Red molecule (see Fig. 17c for its chemical structure). The coupling between Ca and Fura-Red shifts the excitation and emission spectra of the latter molecule (such fluorophores are

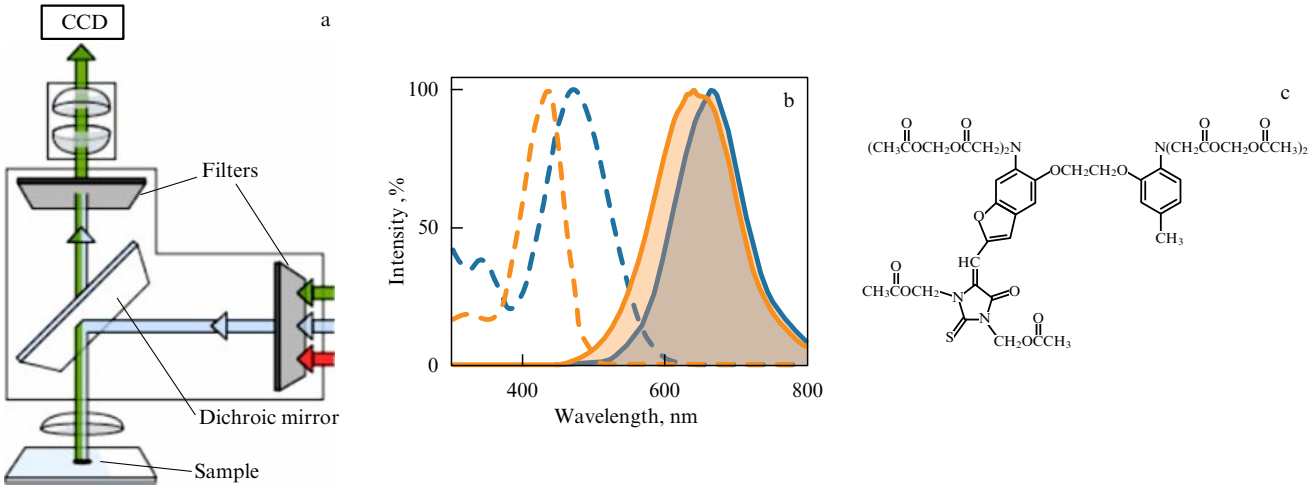

Figure 17. (Color online.) (a) Layout of a fluorescence microscope, (b) Excitation (dashed curve) and emission (solid curve) spectra of Fura-Red in calcium-bound (orange curve) and free (blue curve) states. (c) The chemical structure of a Fura-Red molecule.

called ratiometric). Figure 17b shows excitation and emission spectra (the dashed and solid curves, respectively) of calcium-bound (orange curve) and free Fura-Red molecules (blue curve). The calcium concentration in the cell is calculated from the ratio of fluorescence intensities at two wavelengths, λ_1 and λ_2. To recalculate ratiometric intensity of fluorophore emission into the intracellular concentration of calcium, the following formula is used [61]:

$$[Ca^{2+}] = \beta K_d \frac{R - R_{min}}{R_{max} - R},$$

where R is the ratio of fluorescence intensities of the radiometric probe at the λ_1 wavelength to that at λ_2; R_{min} and R_{max} are maximum and minimal relative fluorescence intensities of the staining dye; K_d is the probe dissociation constant; and β is the normalization factor equal to the ratio of probe intensities at zero and saturating calcium concentrations.

Fura-Red molecules enter the cell through the following route. Carboxyl groups of Fura-Red are modified by acetoxymethyl ether groups, which yields uncharged hydrophobic molecules capable of crossing the lipid bilayer of the plasma membrane. Once Fura-Red is in the cell, intracellular proteins (esterases) cut off its lipophilic groups, thus making the molecule charged and unable to pass through lipid membranes.

Fura-2 belongs to a different class of calcium-binding fluorophores. Binding does not shift its emission spectra but causes a several-fold rise in fluorescence intensity (such fluorophores are termed nonratiometric). In this case, calcium concentration in the cell is calculated from variations in fluorophore fluorescence intensity. Fura-2 enters the cell by the same route as Fura-Red. Calcium concentration in a cell containing a nonratiometric fluorophore is given by the formula [61]

$$[Ca^{2+}] = K_d \frac{F - F_{min}}{F_{max} - F},$$

where F is the fluorescence intensity of the nonratiometric probe, and F_{min} and F_{max} are the minimum and maximum dye fluorescence levels.

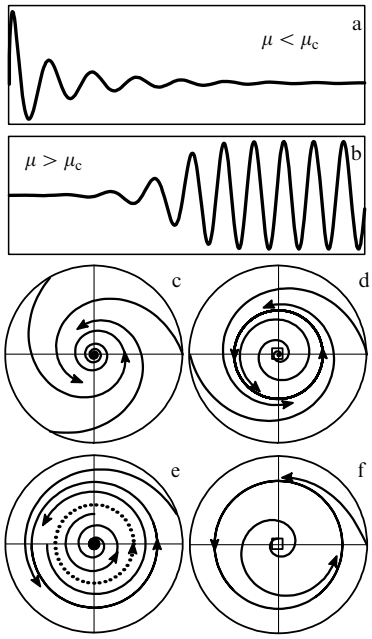

Figure 18. (a) Exponentially decaying oscillations, (b) growing oscillation amplitude, (c, d) soft excitation of oscillations, (e, f) hard excitation of oscillations.

Appendix 2. Poincaré–Andronov–Hopf bifurcation

Let us assume that a certain system comes to equilibrium via exponentially damping oscillations (Fig. 18a); in other words, a minor perturbation in the system decays after short-term oscillations. Suppose, further, that the oscillation damping rate depends on parameter μ. If the change of μ leads to a decrease of the damping, then at a certain bifurcation value μ_c the damping gives way to increase of the oscillation amplitude (Fig. 18b). If in this case the amplitude grows to a certain maximum value, it is said that Poincaré–Andronov–Hopf bifurcation occurred in the system. In terms of phase flows, PAHB occurs when the stable focus (Fig. 18c) is replaced by an unstable one around which a stable limit cycle forms (Fig. 18c).

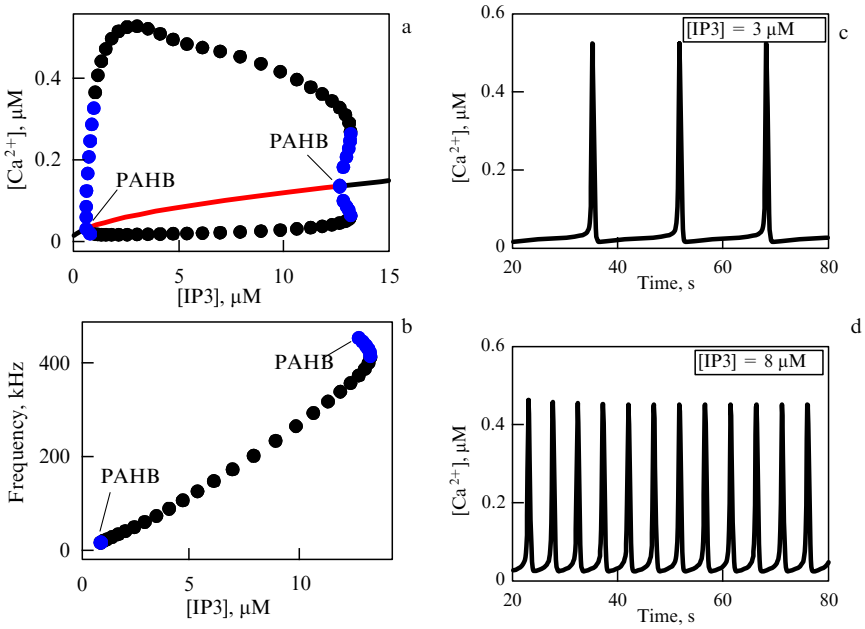

Figure 19. (Color online.) (a) Model bifurcation diagram. Solid black curve shows stable equilibrium position of the system, red curve unstable equilibrium position, blue dots the amplitude of unstable calcium oscillations, black dots the stable oscillation amplitude. At the beginning, PAHB and hard excitation of calcium concentration oscillations occur. A rise in the IP3 level induces one more bifurcation, the unstable limit cycle expands and absorbs the stable one, after which oscillations become damping. (b) Dependence of calcium concentration oscillation frequency on the IP3 level. Examples of calcium concentration oscillations at IP3 concentrations of 3 μM (c) and 8 μm (d).

Excitations of oscillations described above are called soft (Figs 18c, d). Hard excitation is equally possible (Figs 18e, f). In the latter case, two limit cycles develop: one stable, the other unstable nested in the former. A stable singular point can exist within this pair of limit cycles. As the parameter approaches a bifurcation value, the unstable limit cycle shrinks to the focus. If the parameter has a bifurcation value, the stable focus becomes unstable due to the presence of the unstable limit cycle (the dotted curve in Fig. 18e), and the large stable limit cycle remains the sole attractor. In this case, large-amplitude oscillations are excited in a stepwise fashion.

Appendix 3. Sophisticated model of calcium oscillations

The sophisticated calcium oscillation model described in [40] suggests that the cell is open to calcium, which leads to the appearance of two flows, J_{PMCA} and J_{in}. J_{PMCA} denotes calcium flow from the cytosol to the external medium against the concentration gradient through the plasma membrane. This flow is driven by PMCA pumps. The dependence of PMCA operation speed on calcium concentration resembles that for SERCA (Fig. 5b):

$$J_{\mathrm{PMCA}} = \frac{V_{\mathrm{p}} c^2}{K_{\mathrm{p}}^2 + c^2},$$

where $V_{\mathrm{p}} = 2.8\ \mu\mathrm{M}^{-1}\ \mathrm{s}^{-1}$, $K_{\mathrm{p}} = 0.425\ \mu\mathrm{M}$.

The J_{in} flow is formed by calcium flows from the external medium into the cell via Ca channels and Ca leakage: $J_{\mathrm{in}} = J_{\mathrm{chan}} + J_{\mathrm{leakP}}$. It is known that many calcium channels open when the IP3 level increases and allow calcium to freely enter the cell along the concentration gradient. It is usually assumed that the flow rate through these channels linearly depends on the IP3 level. Then, together with leakage (normally constant),

$$J_{\mathrm{in}} = q_1 + q_2 p,$$

where $q_1 = 0.003\ \mu\mathrm{M}\ \mathrm{s}^{-1}$, $q_2 = 0.02\ \mathrm{s}^{-1}$.

The dependence of flow through SERCA that varies as well is expressed as

$$J_{\mathrm{SERCA}} = \frac{c - \gamma_1 c_{\mathrm{e}}}{\gamma_2 - \gamma_3 c + \gamma_4 c_{\mathrm{e}} + \gamma_5 c c_{\mathrm{e}}},$$

where $\gamma_1 = 10^{-4}$, $\gamma_2 = 0.007$ s, $\gamma_3 = 0.06\ \mu\mathrm{M}^{-1}$ s, $\gamma_4 = 0.0014\ \mu\mathrm{M}^{-1}$ s, $\gamma_5 = 0.007\ \mu\mathrm{M}^{-2}$ s.

The IP3R receptor dynamics changes significantly too. Sophisticated models take into consideration that this receptor can be present in six different states with various transitions between them. They are R — inactive receptor, O — open receptor, S — closed receptor due to the high calcium concentration, A — activated receptor, I_1 and I_2 — inactivated receptors. The dynamics of transitions between these states is described by the following equations:

$$\frac{\mathrm{d}R}{\mathrm{d}t} = \phi_{-2} O - \phi_2 p R + k_{-1} I_1 - \phi_1 R,$$

$$\frac{\mathrm{d}O}{\mathrm{d}t} = \phi_2 p R - (\phi_{-2} + \phi_4 + \phi_3) O + \phi_{-4} A + k_{-3} S,$$

$$\frac{\mathrm{d}A}{\mathrm{d}t} = \phi_4 O - \phi_{-4} A - \phi_5 A + k_{-1} I_2,$$

$$\frac{\mathrm{d}I_1}{\mathrm{d}t} = \phi_1 R - k_{-1} I_1,$$

$$\frac{\mathrm{d}I_2}{\mathrm{d}t} = \phi_5 A - k_{-1} I_2,$$

where

$$\phi_1 = \frac{\alpha_1 c}{\beta_1 + c}\,, \quad \phi_2 = \frac{\alpha_2 + \beta_2 c}{\beta_1 + c}\,, \quad \phi_3 = \frac{\alpha_3}{\beta_3 + c}\,, \quad \phi_4 = \frac{\alpha_4 c}{\beta_3 + c}\,,$$

$$\phi_5 = \frac{\alpha_5 c}{\beta_5 + c}\,, \quad \phi_{-2} = \frac{\alpha_{-2} + \beta_{-2} c}{\beta_3 + c}\,, \quad \phi_{-4} = \frac{\alpha_{-4}}{\beta_5 + c}\,,$$

$$R + O + S + A + I_1 + I_2 = 1\,,$$

$\alpha_1 = 0.3\ \mathrm{s}^{-1}$, $\alpha_2 = 0.77\ \mathrm{s}^{-1}$, $\alpha_{-2} = 76.6\ \mu\mathrm{M}\ \mathrm{s}^{-1}$, $\alpha_3 = 6\ \mathrm{s}^{-1}$, $\alpha_4 = 4926\ \mathrm{s}^{-1}$, $\alpha_{-4} = 1.43\ \mathrm{s}^{-1}$, $\alpha_5 = 1.78\ \mathrm{s}^{-1}$, $\beta_1 = 0.02\ \mu\mathrm{M}$, $\beta_2 = 1.38\ \mu\mathrm{M}^{-1}\ \mathrm{s}^{-1}$, $\beta_{-2} = 137\ \mathrm{s}^{-1}$, $\beta_3 = 54.7\ \mu\mathrm{M}$, $\beta_5 = 0.12\ \mu\mathrm{M}$, $k_{-1} = 0.84\ \mathrm{s}^{-1}$, $k_{-3} = 29.8\ \mathrm{s}^{-1}$.

The calcium dynamics is described by the equations

$$\frac{\mathrm{d}c}{\mathrm{d}t} = J_{\mathrm{IP3R}} + J_{\mathrm{leak}} - J_{\mathrm{SERCA}} + J_{\mathrm{PMCA}} - J_{\mathrm{in}}\,,$$

$$\frac{\mathrm{d}c_{\mathrm{e}}}{\mathrm{d}t} = -\gamma\left(J_{\mathrm{IP3R}} + J_{\mathrm{leak}} - J_{\mathrm{SERCA}}\right),$$

where

$$J_{\mathrm{IP3R}} = k_f(0.1O + 0.9A)^4(c_{\mathrm{e}} - c)\,, \quad J_{\mathrm{leak}} = L_{\mathrm{er}}(c_{\mathrm{e}} - c)\,,$$

$L_{\mathrm{er}} = 0.002\ \mathrm{s}^{-1}$, $\gamma = 5.4$, $k_f = 0.96\ \mathrm{s}^{-1}$ are model parameters.

Figure 19 presents results of calculations in the sophisticated model. The basic elements of calcium concentration oscillations remained unaltered. Activation was due to Poincaré–Andronov–Hopf bifurcation, and a rise in the IP3 level resulted in a higher oscillation frequency.

References

1. Alberts B et al. *Molecular Biology of the Cell* (New York: Garland Science, Taylor and Francis Group, 2015)
2. Clapham D E *Cell* **131** 1047 (2007)
3. Berridge M J, Bootman M D, Roderick H L *Nature Rev. Mol. Cell. Biol.* **4** 517 (2003)
4. Bootman M D *Cold Spring Harbor Perspect. Biol.* **4** a011171 (2012)
5. Berridge M J *J. Physiol.* **586** 5047 (2008)
6. Ross W N *Nature Rev. Neurosci.* **13** 157 (2012)
7. Volterra A, Liaudet N, Savtchouk I *Nature Rev. Neurosci.* **15** 327 (2014)
8. Whitaker M *Physiol. Rev.* **86** 25 (2006)
9. Vig M, Kinet J-P *Nature Immunology* **10** 21 (2009)
10. Varga-Szabo D, Braun A, Nieswandt B *J. Thrombos. Haemostas.* **7** 1057 (2009)
11. Ringer S *J. Physiol.* **4** 29 (1883)
12. Shimomura O, Johnson F H, Saiga Y *J. Cell. Compar. Physiol.* **59** 223 (1962)
13. Ridgway E B, Gilkey J C, Jaffe L F *Proc. Natl. Acad. Sci. USA* **74** 623 (1977)
14. Tsien R Y *Biochemistry* **19** 2396 (1980)
15. Woods N M, Cuthbertson K S, Cobbold P H *Nature* **319** 600 (1986)
16. Berridge M J *Nature* **386** 759 (1997)
17. Michelson A D (Ed.) *Platelets* (London: Academic Press, 2013)
18. Heemskerk J W M, Mattheij N J A, Cosemans J M E M *J. Thrombos. Haemostas.* **11** 2 (2013)
19. Stalker T J et al. *Blood* **121** 1875 (2013)
20. Welsh J D et al. *Blood* **124** 1808 (2014)
21. Tomaiuolo M et al. *Blood* **124** 1816 (2014)
22. Stalker T J et al. *Blood* **124** 1824 (2014)
23. Welsh J D et al. *Blood* **127** 1598 (2016)
24. Agbani E O, Poole A W *Blood* **130** 2171 (2017)
25. Fogelson A L, Neeves K B *Annu. Rev. Fluid Mech.* **47** 377 (2015)
26. Rivera J et al. *Haematologica* **94** 700 (2009)
27. Li Z et al. *Arteriosclerosis Thrombos. Vascular Biol.* **30** 2341 (2010)
28. Kazmierczak J, Kempe S, Kremer B *Curr. Organic Chem.* **17** 1738 (2013)
29. Ataullakhanov F I et al. *Biol. Membrany* **26** 163 (2009)
30. Dupont G *Models of Calcium Signalling* (New York: Springer Science, 2016)
31. Hohendanner F et al. *Front. Pharmacology* **5** 35 (2014)
32. Blackwell K T *J. Neurosci. Meth.* **220** 131 (2013)
33. Manninen T, Havela R, Linne M-L *Front. Comput. Neurosci.* **12** 14 (2018)
34. Dupont G et al. *Biochim. Biophys. Acta* **1498** 134 (2000)
35. Slaby O, Lebiedz D *Biophys. J.* **96** 417 (2009)
36. Atri A et al. *Biophys. J.* **65** 1727 (1993)
37. Sveshnikova A N, Ataullakhanov F I, Panteleev M A *Mol. Biosyst.* **11** 1052 (2015)
38. Rink T J, Sage S O *Annu. Rev. Physiol.* **52** 431 (1990)
39. Sage S O et al. *J. Thrombos. Haemostas.* **9** 540 (2011)
40. Keener J, Sneyd J, in *Mathematical Physiology* Pt. 1 (Interdisciplinary Applied Mathematics, Vol. 8, Eds J Keener, J Sneyd) (New York: Springer, 2009) p. 273
41. Bezprozvanny I, Watras J, Ehrlich B E *Nature* **351** 751 (1991)
42. Lytton J et al. *J. Biol. Chem.* **267** 14483 (1992)
43. Donahue B S, Abercrombie R F *Cell Calcium* **8** 437 (1987)
44. Sneyd J et al. *Proc. Natl. Acad. Sci. USA* **101** 1392 (2004)
45. De Pittà M et al. *Phys. Rev. E* **77** 030903(R) (2008)
46. De Young G W, Keizer J *Proc. Natl. Acad. Sci. USA* **89** 9895 (1992)
47. Gillespie D T *Annu. Rev. Phys. Chem.* **58** 35 (2007)
48. Gelens L, Huang K C, Ferrell J E (Jr.) *Cell. Rep.* **12** 892 (2015)
49. Balabin F A, Sveshnikova A N *Math. Biosci.* **276** 67 (2016)
50. Murray J D *Mathematical Biology* (New York: Springer, 2002); Translated into Russian: *Matematicheskaya Biologiya* (Moscow–Izhevsk: RKhD, 2009)
51. Oancea E, Meyer T *Cell* **95** 307 (1998)
52. Violin J D et al. *J. Cell Biol.* **161** 899 (2003)
53. Rosse C et al. *Nature Rev. Mol. Cell Biol.* **11** 103 (2010)
54. Kupzig S, Walker S A, Cullen P J *Proc. Natl. Acad. Sci. USA* **102** 7577 (2005)
55. Cullen P J, Lockyer P J *Nature Rev. Mol. Cell Biol.* **3** 339 (2002)
56. Magnus G, Keizer J *Am. J. Physiol.* **273** C717 (1997)
57. Pokhilko A V, Ataullakhanov F I, Holmuhamedov E L *J. Theor. Biol.* **243** 152 (2006)
58. Shakhidzhanov S S et al. *Biochim. Biophys. Acta* **1850** 2518 (2015)
59. Obydennyy S I et al. *J. Thrombos. Haemostas.* **14** 1867 (2016)
60. Sveshnikova A N et al. *J. Thrombos. Haemostas.* **14** 2045 (2016)
61. Rudolf R et al. *Nature Rev. Mol. Cell Biol.* **4** 579 (2003)